

Critical differences in the surface electronic structure of Ge(001) and Si(001): *Ab initio* theory and angle-resolved photoemission spectroscopy

Hosung Seo, Richard C. Hatch, Patrick Ponath, Miri Choi, Agham B. Posadas, and Alexander A. Demkov*

Department of Physics, The University of Texas at Austin, Austin, Texas 78712, USA

(Received 12 September 2013; revised manuscript received 9 March 2014; published 27 March 2014)

Even with renewed interest in Ge as a competitor to Si in field-effect transistors, several key features of the surface electronic structure of Ge(001) have remained controversial. Notably, the origin of strong Fermi-level pinning in Ge has been heavily debated. Using high-resolution angle-resolved photoemission spectroscopy (ARPES) and first-principles hybrid density functional theory calculations, we compare and unambiguously establish the critical differences between the electronic structure of the Si and Ge (001) surfaces. We explicitly show that the surface state that determines the charge neutrality level, and thus the Schottky barrier height in Si, is actually a surface resonance in Ge. It means that the evanescent states near the Ge surface play an essential role in the strong Fermi-level pinning. Additionally, we identify the origin of a number of highly debated ARPES features for Ge(001) and Si(001).

DOI: [10.1103/PhysRevB.89.115318](https://doi.org/10.1103/PhysRevB.89.115318)

PACS number(s): 71.15.Mb, 68.47.Fg, 79.60.-i

I. INTRODUCTION

As the semiconductor industry searches for alternatives to the Si channel in field-effect transistors, there has recently been a renewed interest in Ge [1–4]. The electron and hole mobilities in Ge are not only higher than in their cousin, Si, but also closer in magnitude, both of which make Ge a very promising replacement [1,5]. With the current trend in the semiconductor industry toward the use of high- k dielectrics [6–8], Ge(001) has an additional advantage; Ge is much less reactive with oxygen and can form a more stable interface with many large-permittivity (high- k) dielectrics. Recently, however, it has been found that Ge strongly pins the Fermi level at the charge neutrality level, less than 0.1 eV above the valence-band top (VBT), which may explain the poor performance of Ge n -type metal-oxide-semiconductor field-effect transistor n MOSFET [9]. The Fermi-level pinning (FLP) and the Schottky barrier are two important properties that must be understood for channel materials used in complementary metal-oxide-semiconductor (CMOS) technology [10,11]. However, the origin of the strong FLP found on the Ge(001) surface/interface has been heavily debated [12–15]. The main question is whether the state pinning the Fermi level is a bulk evanescent state or a surface/interface state. Tsipas and Dimoulas considered the dangling-bond states to model the FLP in Ge [12], but the position of the dangling-bond states is, itself, rather controversial [16,17]. On the other hand, Nishimura *et al.* have suggested that the strong FLP is related to an intrinsic property of the Ge bulk, implying the source of the pinning is evanescent states [13,18]. To understand the FLP in Ge(001), it is crucial to have a clear picture of the surface electronic structure.

The electronic properties of the Ge(001) and Si(001) surfaces have been investigated experimentally [19–34] and theoretically [29,32–40]. However, compared to our excellent understanding of the electronic properties of the Si(001) surface, a similar level of understanding of the Ge(001) surface properties has remained elusive. For Si(001), it has been

established that the dimer-derived surface state maintains its surface character in the fundamental gap, and even at the VBT, thus playing a crucial role in determining the charge neutrality level and FLP [10]. Unfortunately, the character of the Ge(001) VBT and the behavior of the surface states near the VBT has not been well established [21,26,28–33,40]. From photoemission experiments, Kipp *et al.* suggested that the highest valence state originates from the up atom of a dimer [26], while Nakatsuji *et al.* concluded that the VBT is a bulk state [29]. Using density functional theory (DFT), Radny *et al.* argued that the VBT is comprised exclusively of the back-bond states [32]. Subsequently, Yan *et al.* showed if the Ge(001) slab thickness is increased, the character of the VBT becomes bulklike [40]. Unfortunately, additional increases in slab thickness cause the valence and conduction bands to overlap [33] because both the local density approximation (LDA) and the generalized gradient approximation (GGA) underestimate the band gap [41]. With these theories predicting an overlap of the valence and conduction bands, it has been impossible to describe the nature of the Ge VBT and the surface-state behavior inside the gap, thus rendering a charge neutrality level analysis for Ge(001) problematic.

In this paper, we report a combined theoretical and experimental investigation of the surface electronic structure of Ge(001) and Si(001). By comparing our angle-resolved photoemission spectroscopy (ARPES) data to the theoretical spectral functions, we show that the VBT of Ge(001) is exclusively a bulk state. This behavior is unlike the case of Si where the surface state maintains its localized character, even at the VBT. Because the Si surface state resides above the VBT it plays a crucial role in determining the FLP. The equivalent surface state in Ge actually joins the valence band and becomes strong surface resonance just below the Ge VBT. These results show that the FLP at Ge(001) indeed originates from the evanescent states [9,13,18].

II. COMPUTATIONAL AND EXPERIMENTAL DETAILS

In order to avoid the problems associated with the band-gap underestimation in local-density approximation (LDA)

*demkov@physics.utexas.edu

and generalized-gradient approximation (GGA), we utilized the screened Hartree-Fock hybrid functional due to Heyd, Scuseria, and Ernzerhof (HSE06) [42], within the projector augmented wave method [43], as implemented in the VASP code [44,45] used in this work. Further theoretical details are described in the Supplemental Material [46]. In HSE06, we checked that the band gap of Ge is reproduced within 3% of experiment [47–49], which means we can make accurate predictions about the character of the Ge VBT.

The samples and preparation of the Ge(001)- 2×1 and Si(001)- 2×1 surfaces have been described in detail elsewhere [50–52]. Unlike previous ARPES experiments, where the Ge(001) surfaces were prepared using cycles of ion sputtering and annealing, our Ge(001) surfaces were prepared using a combination of wet etching and oxygen plasma cleaning. This technique has the advantage of avoiding the incomplete healing of the surface roughening associated with sputtering and annealing cycles [53]. Sample preparation and analysis were performed *in situ* as described elsewhere [51,52,54]. All ARPES experiments were performed at room temperature, with a total energy resolution of $\Delta E < 30$ meV and an angular resolution of $\Delta\theta < 1^\circ$. A monochromated He discharge lamp was used with excitation energies of $h\nu = 21.22$ eV and $h\nu = 40.81$ eV.

III. RESULTS AND DISCUSSIONS

The surface band structures of Si(001) and Ge(001) in GGA [46,55] are shown in Figs. 1(a) and 1(b), respectively. Notably present in the fundamental gaps of Ge and Si are the intrinsic surface states. For the Si(001) band structure, the solitary band

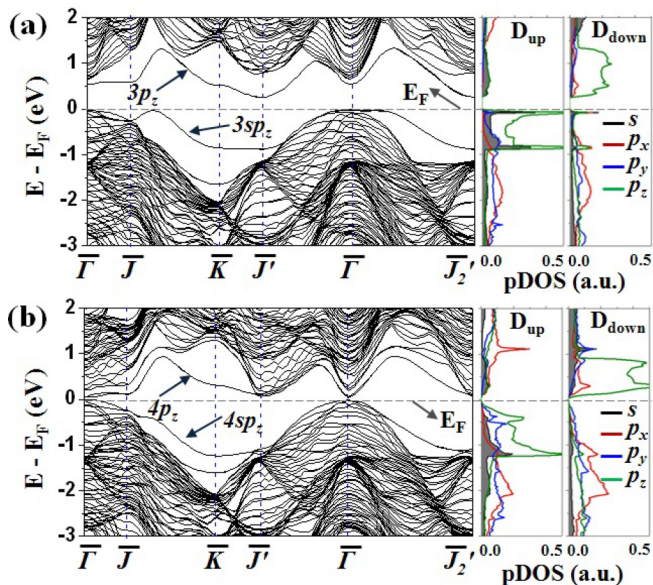


FIG. 1. (Color online) The surface band structure for Si(001)- 2×1 (a) and Ge(001)- 2×1 (b) as calculated in GGA, including orbital projected density of states (pDOS). The 2×1 surface Brillouin zone whose orientation with respect to the bulk zone is shown in the Supplemental Material [46]. For the orbital pDOS, we project the total DOS on the up (denoted as D_{up}) and down (denoted as D_{down}) atoms of a surface dimer [46].

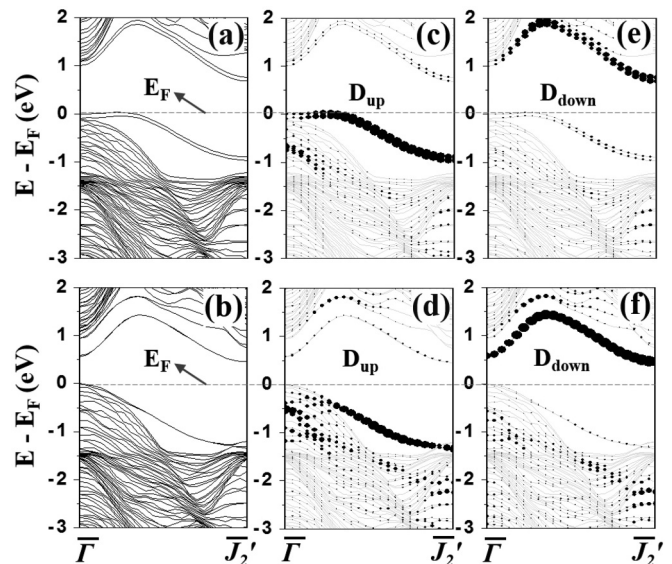


FIG. 2. HSE06 surface band structures of Si(001)- 2×1 (a) and Ge(001)- 2×1 (b). The surface bands are doubled since the slab has the dimer structure on both surfaces. The band structures (light gray) weighted with the wave-function character derived from the D_{up} atom [(c) for Si and (d) for Ge] and the D_{down} atom [(e) for Si and (f) for Ge] are shown.

right above (below) the Fermi level is derived from the down (up) atom of the surface dimer, and is denoted as D_{down} (D_{up}). Similar features are also found for Ge(001). For the Ge(001) slab band structure we find a small band gap of 0.05 eV at $\bar{\Gamma}$. This is due to the quantum confinement effect originating from the finite slab thickness. However, for the extended surface reconstructions such $c(2 \times 4)$ and $p(2 \times 2)$, the surface gap of Ge(001) at $\bar{\Gamma}$ is completely closed in GGA. We checked that no significant changes for the surface band structure of Si(001) and Ge(001) are induced by the spin-orbit coupling [56] at the GGA functional level.

Figures 2(a) and 2(b) show the HSE06 surface band structure of Si(001) and Ge(001)- 2×1 surfaces from $\bar{\Gamma}$ to \bar{J}_2' , respectively. We first note the bulk band gap of Si(001) and Ge(001), at $\bar{\Gamma}$, corresponds to the indirect gap of the Si bulk and the direct gap of the Ge bulk, respectively, as all the bulk levels along ΓX (the y direction) are projected on the surface Brillouin zone in the slab calculations [46]. We calculate the bulk gap at $\bar{\Gamma}$ to be 1.18 and 0.94 eV for Si(001) and Ge(001), respectively, which agree well with the previous theoretical bulk calculations [48,49] and the experimental values of 1.17 and 0.90 eV for the bulk Si and Ge, respectively [47]. Additionally, we find the unoccupied Si(001) and Ge(001) D_{down} surface states at $\bar{\Gamma}$ are positioned 1.1 and 0.6 eV above the bulk VBT, respectively. For Ge(001), inverse photoemission spectroscopy reported the empty D_{down} state to be 0.6 eV [24] or 0.85 eV [39] above the VBT at $\bar{\Gamma}$, while that of Si(001) was estimated to be 1.1 eV using optical absorption spectroscopy data [38,57]. Our theoretical results are in excellent agreement with these experimental values.

In Fig. 3(a), we show the ARPES spectrum of Ge(001)- 2×1 measured along the $\bar{\Gamma}\bar{J}_2'$ direction [29,46]. For comparison with theory, we also plot the spectral functions of

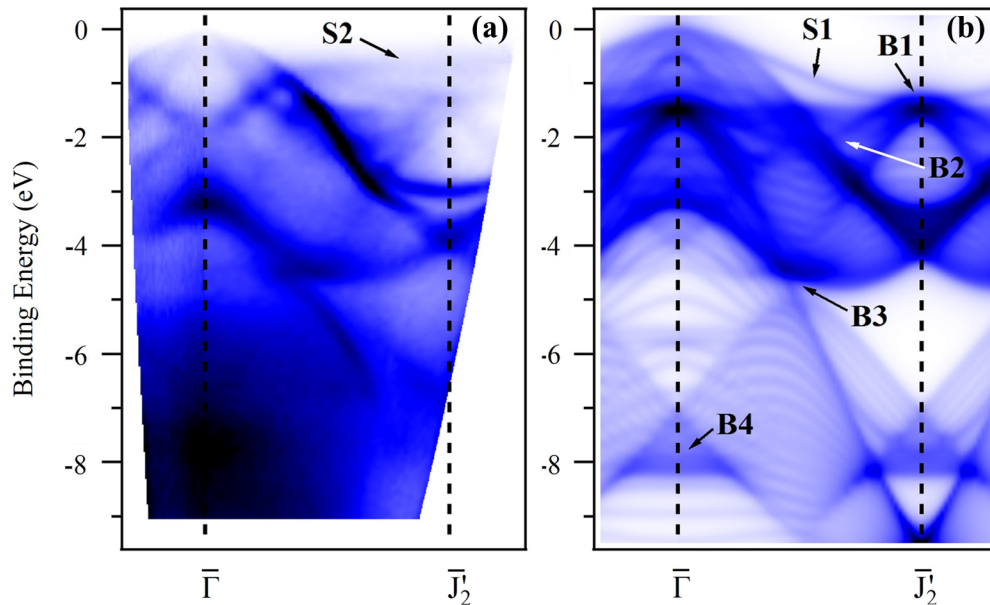


FIG. 3. (Color online) ARPES spectrum of Ge(001)- 2×1 measured using a photon energy of 21.22 eV (a), compared with the theoretical spectral function calculated in HSE06 (b).

Ge(001)- 2×1 in Fig. 3(b), as calculated in HSE06 [46]. Virtually all important features observed experimentally are well reproduced in theory. First of all, by comparing slab and bulk calculations, we find that most features in Fig. 3(b), other than S1, are mainly derived from bulk states. The bulk features such as B1-B4 appear strong because they have less k_z dependence, and thus account for features in ARPES data. The S1 state halfway between $\bar{\Gamma}$ and \bar{J}_2 is in the fundamental energy gap and is a surface state. This state is also seen experimentally, with excellent agreement on the dispersion. Most importantly, the Ge S1 state becomes degenerate with the bulk states and therefore becomes a surface resonance as it approaches $\bar{\Gamma}$ [29], while the corresponding band in Si(001) is a true surface state, even at $\bar{\Gamma}$, as shown in Fig. 2(a). Additionally, we note that ARPES shows the surface state splitting into two bands, of which the top one [S2 in Fig. 3(a)] is not reproduced by theory. The same splitting is also observed in our Si(001)- 2×1 measurements (not shown) and in the literature [23,27]. This S2 band is likely a result of the anti-phase-flipping motion of the dimers along the (1-1 0) direction [23], and we verified that a similar splitting of the surface state occurs for the $p(2 \times 2)$ - and $c(2 \times 4)$ -reconstructed surfaces.

To shed more light on the surface resonance features in Ge(001), we show the projection of the valence wave functions on the up atom of a dimer, for Si(001) and Ge(001), in Figs. 2(c) and 2(d), respectively. While D_{up} in Si(001) shows a strongly localized character (true surface state in the fundamental gap), D_{up} in Ge(001) acquires a stronger surface resonance character near $\bar{\Gamma}$ as it strongly mixes with the bulk states. The strong surface resonance in Ge(001) leads to two additional spectral features at $\bar{\Gamma}$ that are located at -0.5 and -1.2 eV [see Fig. 2(d)]. Experimentally, it has been shown that these two states do not disperse as a function of photon energy [20,21], but it has been heavily debated whether these states are surface resonances [35]. Our calculations shown in Fig. 2(d) confirm that the experimentally observed spectral features located at

$\bar{\Gamma}$ and at ~ -0.6 and -1.2 eV [20,21] originate from surface resonances. We have also studied these features in GGA [46]. For the Si(001)- 2×1 surface, normal-emission spectra reveal two states at $\bar{\Gamma}$ that do not disperse with photon energy: one very close to the VBT and the other one at -0.8 ± 0.1 eV, whose origin has been unclear [22]. According to our calculations shown in Fig. 2(c), the one near the VBT is the surface-state feature corresponding to the D_{up} state at $\bar{\Gamma}$. We also observe a surface resonance feature at -0.7 eV [see Fig. 2(c)], which is in excellent agreement with experiment [22].

To better understand the behavior of the surface states in Si(001) and Ge(001), we note that, due to the tilting of the dimer [10,58], the dangling hybrid on the down atom becomes almost p_z -like and the up atom gains increased s character [see Figs. 1(a) and 1(b)]. This tilting of dimers lowers its average energy. Using all-electron atomic density functional theory (DFT) calculations [59], we find that the Si $3p$ level and the Ge $4p$ level are well aligned and close in energy, but the Ge $4s$ level drops in energy more than the Si $3s$ level [58]. In the scalar relativistic approximation, the sp splittings in Si and Ge are calculated to be 6.71 and 7.88 eV, respectively. Using the Dirac-Kohn-Sham equation, the difference between the $4p_{3/2}$ and $4s_{1/2}$ states in Ge is further increased to 7.93 eV, while that of Si is 6.72 eV. As a result, both GGA and HSE06 surface band structure calculations (Figs. 1 and 2) show the occupied surface state of Ge ($4sp_z$) dropping in energy more than that of Si ($3sp_z$).

Despite the overall agreement between experiment and theory seen in Fig. 3, we note that there are a number of detailed features which are not captured in the slab calculations. These include the three bands found in ARPES measurements for the VBT of Ge(001) [29], which are clearly shown in Fig. 4(a) (labeled E_1 , E_2 , and SR). The main reason why this three-band feature is not captured in the slab calculations is that the surface band structure shown in Fig. 2(b) is, essentially, a projection of all the bulk bands onto the surface Brillouin zone. ARPES

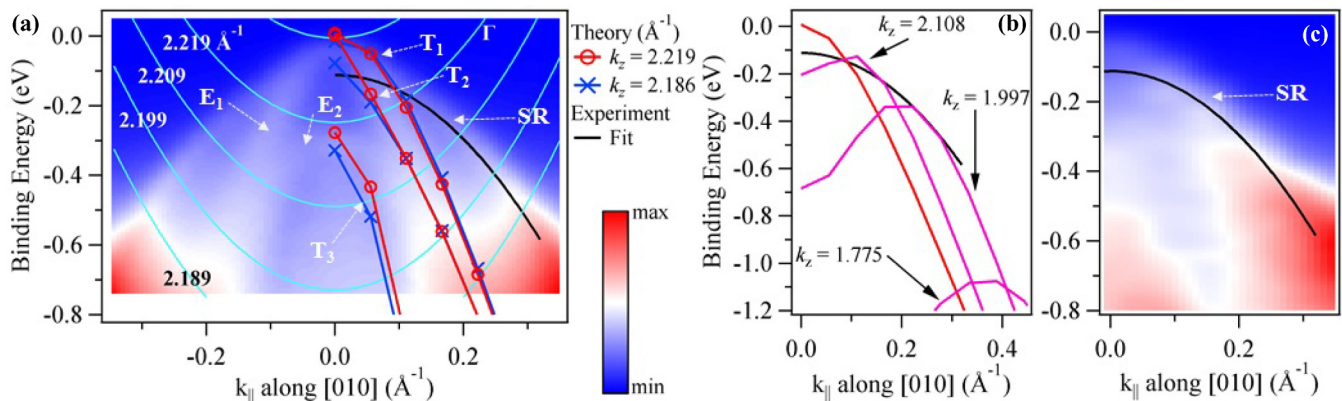


FIG. 4. (Color online) (a) ARPES spectrum of Ge(001) VBT measured with a photon energy of $h\nu = 21.22$ eV, with theoretical bulk bands (T_1 – T_3) for $k_z = 2.186$ and 2.219 \AA^{-1} overlaid. Experimental bands are labeled E_1 , E_2 , and SR (surface resonance). Also shown are constant k_z contours indicating this spectrum very nearly corresponds to the bulk Γ point. (b) Theoretical T_1 bulk bands for k_z from 2.219 to 1.775 \AA^{-1} , as well as the fit to the SR band in (a) which shows precisely how this state merges with the bulk valence band. (c) ARPES spectrum of Ge(001) VBT measured with the photon energy of $h\nu = 40.81$ eV. The black line is a fit to the dispersion of the SR feature from (a) and shows that despite a large change in k_z , the state hardly disperses.

experiments, on the other hand, contain only a small range of k_z values, as seen by the constant k_z contours (determined using a free-electron final-state model [46,60–63]) shown in Fig. 4(a).

In order to determine the origin of the two lighter bands, we performed a number of bulk calculations along $\overline{\Gamma J_2}$ using HSE06 with and without spin-orbit coupling [56]. When $k_z = 2.219$ \AA^{-1} , this is equivalent to calculating the band structure from Γ to X . Calculations reveal three bulk bands that are spin-orbit split-off p bands, for k_z values near the Γ point ($k_z = 2.219$ \AA^{-1}), as plotted on top of the ARPES data in Fig. 4(a) and labeled T_1 – T_3 . These theoretically predicted bands are in good agreement with the experimental data, especially in terms of the theoretical spin-orbit splitting of 0.28 eV. We also show that for a range of wave-vector values spanning most of the ARPES data in Fig. 4(a) (i.e., $k_z = 2.219 \pm 0.02$ \AA^{-1}) [46], T_1 – T_3 hardly disperse and explain the well-defined bulk bands observed experimentally for $h\nu = 21.22$ eV.

This model analysis suggests that the heavy-hole band (SR) observed in Fig. 4(a) is a surface-related band, which is further supported by the ARPES measurements performed with the higher photon energy shown in Fig. 4(c) [46]. By using a photon energy of $h\nu = 40.81$ eV, the k_z range for the ARPES measurements of the VBT is shifted to $k_z = 2.845 \pm 0.03$ \AA^{-1} (i.e., roughly half way between the Γ and X points of the bulk Brillouin zone [46]). For this range of k_z there are no bulk states in the binding energy range of Fig. 4(c). As expected, the two light bands ($E_{1,2}$) observed for $h\nu = 21.22$ eV are not present in Fig. 4(c). However, the heavy band is still present with much the same dispersion—a clear indication that this band is heavily surface related. This surface resonance becomes a true surface state (S1) where it gives rise to the strong spectral feature observed at $k_{\parallel} \approx 0.3$ \AA^{-1} .

Despite using the most advanced theoretical methods, it should be noted that there are discrepancies between the ARPES data and theory. While the spin-orbit splitting and overall bandwidths show excellent agreement between experiment and theory [see Figs. 3(a), 3(b), and 4(a)], it is

somewhat surprising that there is not better agreement in the dispersion of the experimental band E_2 and theoretical band T_3 . While some of this discrepancy could be attributed to the finite k_z range measured in the ARPES spectra, it cannot completely account for the differences, and should be further investigated.

IV. CONCLUSION

In summary, we unambiguously identify the key features of the Ge(001) surface electronic structure in comparison with the Si(001) surface. We show that the surface state of Ge(001) becomes a surface resonance as it approaches the $\overline{\Gamma}$ point and the state at the valence-band top is exclusively a bulk state. The theoretical spectral features originating from the strong surface resonance in Ge(001) are in excellent agreement with experimental observations and also answer long-standing questions concerning the electronic structure and ARPES data for the Ge(001) surface. Furthermore, our results imply that the Ge surface state, unlike that in Si, is not important for the Schottky barrier analysis, but the evanescent states in the fundamental energy gap play a critical role in determining the charge neutrality level, and the Fermi-level pinning in Ge. In addition to providing a deeper understanding of the fundamental properties of semiconductor surfaces, these results should inspire further theoretical and experimental research relating to the feasibility of advancing the use of the Ge(001) surface in transistor technology.

ACKNOWLEDGMENTS

H.S. gratefully acknowledges support through The University of Texas at Austin William Powers, Jr., Presidential Fellowship. This work was supported by the Air Force Office of Scientific Research under Grant No. FA9550-12-1-0494, Office of Naval Research under Grant No. N000 14-10-1-0489, and the Texas Advanced Computing Center.

- [1] R. Pillarisetty, *Nature* **479**, 324 (2011).
- [2] G. Scappucci, O. Warschkow, G. Capellini, W. M. Klesse, D. R. McKenzie, and M. Y. Simmons, *Phys. Rev. Lett.* **109**, 076101 (2012).
- [3] S. Paleari, S. Baldovino, A. Molle, and M. Fanciulli, *Phys. Rev. Lett.* **110**, 206101 (2013).
- [4] K. C. Saraswat, C. O. Chui, T. Krishnamohan, A. Nayfeh, and P. McIntyre, *Microelectron. Eng.* **80**, 15 (2005).
- [5] H. Shang, H. Okorn-Schmidt, K. K. Chan, M. Chopel, J. A. Ott, P. M. Kozlowski, S. E. Steen, S. A. Cordes, H.-S. P. Wong, E. C. Jones, and W. E. Haensch, *Electron Devices Meeting, 2012, IEDM'02. International* (IEEE, San Francisco, 2002), pp. 441–444.
- [6] L. Zhang, M. Gunji, S. Thombare, and P. C. McIntyre, *IEEE Electron Device Lett.* **34**, 732 (2013).
- [7] R. Zhang, T. Iwasaki, N. Taoka, M. Takenaka, and S. Takagi, *IEEE Trans. Electron Devices* **59**, 335 (2012).
- [8] J. J. Gu, Y. Q. Liu, M. Xu, G. K. Celler, R. G. Gordon, and P. D. Ye, *Appl. Phys. Lett.* **97**, 012106 (2010).
- [9] A. Dimoulas, P. Tsipas, A. Sotiropoulos, and E. K. Evangelou, *Appl. Phys. Lett.* **89**, 252110 (2006).
- [10] H. Lüth, *Solid Surfaces, Interfaces and Thin Films* (Springer-Verlag, Berlin, Heidelberg, 2001).
- [11] W. Mönch, *Semiconductor Surfaces and Interfaces* (Springer-Verlag, Berlin, Heidelberg, 2001).
- [12] P. Tsipas and A. Dimoulas, *Appl. Phys. Lett.* **94**, 012114 (2009).
- [13] T. Nishimura, K. Kita, and A. Toriumi, *Appl. Phys. Lett.* **91**, 123123 (2007).
- [14] D. Kuzum, K. Martens, T. Krishnamohan, and K. C. Saraswat, *Appl. Phys. Lett.* **95**, 252101 (2009).
- [15] K. Kasahara, S. Yamada, K. Sawano, M. Miyao, and K. Hamaya, *Phys. Rev. B* **84**, 205301 (2011).
- [16] J. R. Weber, A. Janotti, P. Rinke, and C. G. Van de Walle, *Appl. Phys. Lett.* **91**, 142101 (2007).
- [17] P. Broqvist, A. Alkauskas, and A. Pasquarello, *Phys. Rev. B* **78**, 075203 (2008).
- [18] J. Tersoff, *Phys. Rev. B* **30**, 4874 (1984).
- [19] D. E. Eastman and W. D. Grobman, *Phys. Rev. Lett.* **28**, 1378 (1972).
- [20] J. G. Nelson, W. J. Gignac, R. S. Williams, S. W. Robey, J. G. Tobin, and D. A. Shirley, *Phys. Rev. B* **27**, 3924 (1983); *Surf. Sci.* **131**, 290 (1983).
- [21] T. C. Hsieh, T. Miller, and T.-C. Chiang, *Phys. Rev. B* **30**, 7005 (1984).
- [22] L. S. O. Johansson, P. E. S. Persson, U. O. Karlsson, and R. I. G. Uhrberg, *Phys. Rev. B* **42**, 8991 (1990).
- [23] Y. Enta, S. Suzuki, and S. Kono, *Phys. Rev. Lett.* **65**, 2704 (1990).
- [24] J. E. Ortega and F. J. Himpsel, *Phys. Rev. B* **47**, 2130 (1993).
- [25] E. Landemark, C. J. Karlsson, L. S. O. Johansson, and R. I. G. Uhrberg, *Phys. Rev. B* **49**, 16523 (1994).
- [26] L. Kipp, R. Manzke, and M. Skibowski, *Surf. Sci.* **269**, 854 (1992); *Solid State Commun.* **93**, 603 (1995).
- [27] C. C. Hwang, T.-H. Kang, K. J. Kim, B. Kim, Y. Chung, and C.-Y. Park, *Phys. Rev. B* **64**, 201304(R) (2001).
- [28] O. Gurlu, H. J. W. Zandvliet, and B. Poelsema, *Phys. Rev. Lett.* **93**, 066101 (2004).
- [29] K. Nakatsuji, Y. Takagi, F. Komori, H. Kusunohara, and A. Ishii, *Phys. Rev. B* **72**, 241308 (2005).
- [30] C. Jeon, C. C. Hwang, T.-H. Kang, K.-J. Kim, B. Kim, Y. Chung, and C. Y. Park, *Phys. Rev. B* **74**, 125407 (2006).
- [31] P. E. J. Eriksson, M. Adell, K. Sakamoto, and R. I. G. Uhrberg, *Phys. Rev. B* **77**, 085406 (2008).
- [32] M. W. Radny, G. A. Shah, S. R. Schofield, P. V. Smith, and N. J. Curson, *Phys. Rev. Lett.* **100**, 246807 (2008).
- [33] M. W. Radny, G. A. Shah, S. R. Schofield, P. V. Smith, and N. J. Curson, *Phys. Rev. Lett.* **103**, 189702 (2009).
- [34] K. Tomatsu, K. Nakatsuji, M. Yamada, F. Komori, B. Yan, C. Yam, T. Frauenheim, Y. Xu, and W. Duan, *Phys. Rev. Lett.* **103**, 266102 (2009).
- [35] P. Krüger, A. Mazur, J. Pollmann, and G. Wolfgarten, *Phys. Rev. Lett.* **57**, 1468 (1986).
- [36] L. Spiess, A. J. Freeman, and P. Soukiassian, *Phys. Rev. B* **50**, 2249 (1994).
- [37] P. Krüger and J. Pollmann, *Phys. Rev. Lett.* **74**, 1155 (1995).
- [38] M. Rohlfing, P. Krüger, and J. Pollmann, *Phys. Rev. B* **52**, 1905 (1995).
- [39] M. Rohlfing, P. Krüger, and J. Pollmann, *Phys. Rev. B* **54**, 13759 (1996).
- [40] B. Yan, C. Yam, A. L. da Rosa, and T. Frauenheim, *Phys. Rev. Lett.* **103**, 189701 (2009).
- [41] L. J. Sham and M. Schlüter, *Phys. Rev. Lett.* **51**, 1888 (1983).
- [42] J. Heyd, G. E. Scuseria, and M. Ernzerhof, *J. Chem. Phys.* **118**, 8207 (2003); J. Heyd and G. E. Scuseria, *ibid.* **121**, 1187 (2004); J. Heyd, G. E. Scuseria, and M. Ernzerhof, *ibid.* **124**, 219906 (2006).
- [43] P. E. Blöchl, *Phys. Rev. B* **50**, 17953 (1994).
- [44] G. Kresse and J. Furthmüller, *Phys. Rev. B* **54**, 11169 (1996).
- [45] J. Paier, M. Marsman, K. Hummer, G. Kresse, I. C. Gerber, and J. G. Ángyán, *J. Chem. Phys.* **124**, 154709 (2006).
- [46] See Supplemental Material at <http://link.aps.org/supplemental/10.1103/PhysRevB.89.115318> for computational and experimental details.
- [47] O. Madelung, *Semiconductors: Data Handbook*, 3rd ed. (Springer, New York, 2004).
- [48] K. Hummer, J. Harl, and G. Kresse, *Phys. Rev. B* **80**, 115205 (2009).
- [49] J. E. Peralta, J. Heyd, G. E. Scuseria, and R. L. Martin, *Phys. Rev. B* **74**, 073101 (2006).
- [50] P. Ponath, A. B. Posadas, R. C. Hatch, and A. A. Demkov, *J. Vac. Sci. Technol. B* **31**, 031201 (2013).
- [51] M. Choi, A. B. Posadas, H. Seo, R. C. Hatch, and A. A. Demkov, *Appl. Phys. Lett.* **102**, 031604 (2013).
- [52] H. Seo, M. Choi, A. B. Posadas, R. C. Hatch, and A. A. Demkov, *J. Vac. Sci. Technol. B* **31**, 04D107 (2013).
- [53] G. Schulze and M. Henzler, *Surf. Sci.* **73**, 553 (1978).
- [54] R. C. Hatch, K. D. Fredrickson, M. Choi, C. Lin, H. Seo, A. B. Posadas, and A. A. Demkov, *J. Appl. Phys.* **114**, 103710 (2013).
- [55] J. P. Perdew, K. Burke, and M. Ernzerhof, *Phys. Rev. Lett.* **77**, 3865 (1996).
- [56] D. D. Koelling and B. N. Harmon, *J. Phys. C: Solid State Phys.* **10**, 3107 (1977).
- [57] Y. J. Chabal, S. B. Christman, E. E. Chaban, and M. T. Yin, *J. Vac. Sci. Technol. A* **1**, 1241 (1983).

- [58] W. A. Harrison, *Electronic Structure and the Properties of Solids* (Dover Publications, Inc., New York, 1989).
- [59] M. J. T. Oliveira and F. Nogueira, *Comput. Phys. Commun.* **178**, 524 (2008).
- [60] X. H. Chen, W. Ranke, and E. Schröder-Bergen, *Phys. Rev. B.* **42**, 7429 (1990).
- [61] T.-C. Chiang, J. A. Knapp, M. Aono, and D. E. Eastman, *Phys. Rev. B* **21**, 3513 (1980).
- [62] F. J. Himpsel, *Appl. Opt.* **19**, 3964 (1980).
- [63] P. Kruse, M. Schowalter, D. Lamoen, A. Rosenauer, and D. Gerthsen, *Ultramicroscopy* **106**, 105 (2006).